Rational shapes of local volatility

The asymptotic behaviour of local volatility surfaces for low and high strikes – the so-called wings – is important in option pricing and risk management. ***Stefano de Marco****,* ***Peter Friz*** *and* ***Stefan Gerhold*** *show certain models allow for the derivation of analytic forms, using saddle-point methods*

Robust implementation of a Dupire-type local volatility model (Dupire, 1994) is important for every equity option trading floor. Typically, this problem is solved in a two-step procedure: a smooth parameterisation of the implied volatility surface; and computation of the local volatility based on the resulting call prices. The first of these, and in particular how to extrapolate the implied volatility in extreme strike regimes, is widely recognised as an important risk management issue, first discussed in the Quant Congress 2000 presentation *Rational shapes of the [implied] volatility surface*. In the Heston stochastic volatility model, implied variance grows asymptotically linearly in log-strike. This and related matters were then studied by numerous authors, starting with Lee (2004). Subsequently, this has inspired parameterisations of the implied volatility surface, notably stochastic-volatility inspired (SVI) parameterisation (see Gatheral, 2006, and Gatheral & Jacquier, 2012).

In this article, we deal with the second step, aiming at an understanding of typical shapes of the local volatility surface, through the behaviour of local volatility at extreme strikes. At the heart of our discussion lies a novel saddle-point-based formula for local volatility that can be used in a wide range of maturities and strikes. When applied to the Heston model, it reveals that local variance is – similar to implied variance – asymptotically linear in log-strike. As an immediate application, this provides a justification for using SVI-type parameterisation for the local variance surface also.

Understanding the local volatility surface in extreme regimes, with robust numerical algorithms, can play an important role in model risk management, for instance when quantifying the model risk attached to a given path-dependent option, subject to consistency with today's vanilla prices. A simple, universally applicable, gauge of model risk is the scale of difference in pricing under stochastic and local volatility models. Of course, it is assumed that both models are calibrated to the same market. Reghai (2011) defines a 'toxicity index' as:

$$I = \frac{|SV - LV|}{|SV + LV|}$$

where SV and LV are the prices of an exotic option under the stochastic and the local volatility models, respectively. A value of I away from zero is a warning flag for a particularly 'toxic', that is, highly model risk-sensitive, product, with all its consequences for hedging decisions.

The trouble with this simple test is that the local volatility in Heston (or other stochastic volatility models) is not explicitly known. Typically, one would then use either Dupire's formula $\sigma^2_{loc}(K, T) = 2\partial_T C/K^2\partial_{KK}C$, with Fourier pricing of the respective derivatives of the call prices, or Monte Carlo-based computation of local variances as conditional expectations, $\sigma^2_{loc}(K, T) = \mathbb{E}[\sigma^2_{stoch}(T)|S_T = K]$. Clearly, if the local volatility price process makes a large move, Dupire's formula cannot be trusted since Fourier pricing is known to become quickly unstable for extreme strikes. Similarly, conditioning on very unlikely events of the form $\{S_T \in [K, K + \delta K]\}$ when $K >> S_0$ is numerically difficult.

These numerical instabilities can be overcome through extrapolation analytics – this article derives results for stochastic volatility of the form $\sigma^2_{loc}(K, T) \sim const.\log K$ for large or small K, known as the surface's wings. The resulting method is straightforward patching: fix a reasonable region I in the (K, T) plane on which local volatility can be reliably calculated with either of the above classical methods and use our approximate formula for a strike-maturity point outside that region. This yields a parametric, globally defined local volatility surface that then serves as the basis of a reliable Monte Carlo simulation for option prices under local volatility.

Let us introduce in some details the mathematical ingredients necessary for the discussion to come. Dupire's formula:

$$\sigma^2_{loc}(K,T) = \frac{2\partial_T C}{K^2\partial_{KK}C} \tag{1}$$

implies that any arbitrage-free call price surface:

$$C = C(K,T) = C_{BS}\left(K,T;\sigma_{BS}(K,T)\right)$$

which arises from an Itô diffusion is also obtained from Dupire's one-factor local volatility model:

$$dS_t / S_t = \sigma_{loc}(S_t,t)dW_t \tag{2}$$

Local volatility can be thought of as a Markovian projection of a higher dimensional model of the form:

$$dS_t / S_t = \sigma_{stoch}(t,\omega)dW_t$$

Indeed, it is known (see, for example, Gatheral, 2006) that:

$$\sigma^2_{loc}(K,T) = \mathbb{E}\left[\sigma_{stoch}(T)^2 \middle| S_T = K\right]$$

But even for stochastic volatility models with fully explicit Markovian specification, sampling from the corresponding local volatility models requires substantial computational effort.

The analysis of implied, local and stochastic volatility and their

A. Monte Carlo bounds

Maturity	Log spot, 10^3 Monte Carlo paths	
	Minimum	Maximum
0.25	–0.71	0.36
1	–1.52	0.59
5	–4.13	1.14

Note: minimum and maximum values of $\log(S_T/S_0)$ attained by a Monte Carlo simulation under Heston local variance (12), with 12 time steps a year and Heston parameters as in figure 4. Even with only 10^3 trajectories, values are reached for which computing local variance by Dupire's formula becomes numerically challenging

1 Local variance for Heston model with Dupire's formula (left wing)

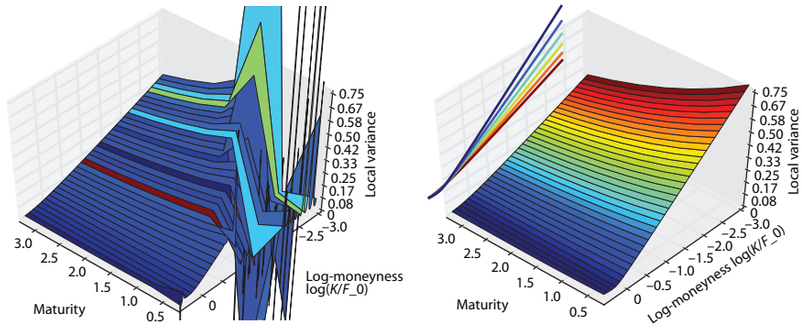

Note: left-hand surface: call price derivatives calculated via one-dimensional integration of Heston characteristic function on a fixed integration contour (here, $0.5 + i\mathbb{R}$). Right-hand surface: on adaptive integration contour with shift into saddle point $\hat{s}(k, T) + i\mathbb{R}$ (see (8)). The ticks and labels of the log-moneyness axis in the left-hand figure (hidden by the numerical oscillations, shown on purpose) are the same as in the right-hand figure; in particular, log-moneyness k ranges from minus three to zero

2 Local variance for Heston model with Dupire's formula (right wing)

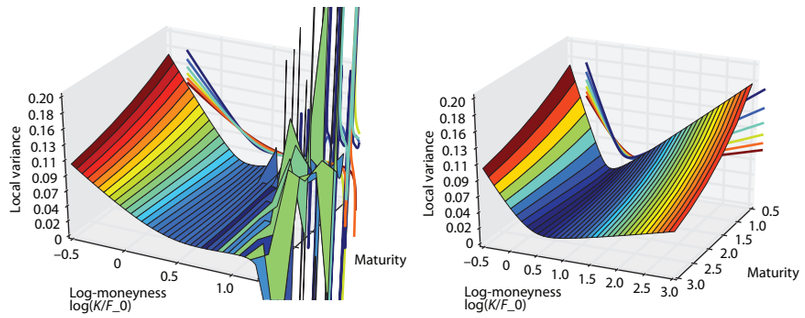

Note: as for figure 1, the ticks and labels of the log-moneyness axis in the left-hand panel are the same as for the right-hand panel; in particular, time ranges from 0.5 to three

interplay has been subject of countless works. Formula (7) below allows for approximation of $\sigma^2_{loc}(K, T)$ when K is large. The main ingredient of this formula is a known moment-generating function (MGF) of the log-price X_t under the pricing measure:

$$M(s,T) := \exp\big(m(s,T)\big) := \mathbb{E}\exp\big(sX_T\big)$$

assumed to be finite in some interval $(s_-(T), s_+(T))$ with critical exponents s_- and s_+ defined as:

$$s_-(T) := \inf\big\{s : M(s,T) < \infty\big\}, \quad s_+(T) := \sup\big\{s : M(s,T) < \infty\big\}$$

We also assume that call prices have sufficient regularity to make Dupire's formula (1) well defined, and that the MGF blows up at the upper critical moment:

$$\lim_{s \uparrow s_+(T)} M(s,T) = \infty \tag{3}$$

This holds, for example, in the Heston model, with log-price $X_t = \log(S_t/S_0)$, where:

$$dS_t = S_t\sqrt{V_t}\,dW_t, \quad S_0 = s_0 > 0,$$
$$dV_t = \big(a + bV_t\big)dt + c\sqrt{V_t}\,dB_t, \quad V_0 = v_0 > 0$$

with $a \geq 0$, $b \leq 0$, $c > 0$, $d\langle W, B\rangle_t = \rho dt$, and we shall assume $\rho \leq 0$, which is typical in equity markets. Before moving on to a more general discussion, we formulate an asymptotic formula for local volatility in the Heston model.

■ **Theorem.** The following asymptotic behaviour of the Heston model's local variance is given by[1]:

$$\lim_{k\to\infty} \frac{\sigma^2_{loc}(k,T)}{k} = \frac{2}{s_+\big(s_+ - 1\big)R_1 / R_2} \tag{4}$$

where $k = \log(K/S_0)$, $s_+ \equiv s_+(T)$ and:

$$\begin{aligned} R_1 = {} & Tc^2 s_+\big(s_+ - 1\big)\Big[c^2\big(2s_+ - 1\big) - 2\rho c\big(s_+\rho c + b\big)\Big] \\ & -2\big(s_+\rho c + b\big)\Big[c^2\big(2s_+ - 1\big) - 2\rho c\big(s_+\rho c + b\big)\Big] \\ & +4\rho c\Big[c^2 s_+\big(s_+ - 1\big) - \big(s_+\rho c + b\big)^2\Big] \end{aligned} \tag{5}$$

$$R_2 = 2c^2 s_+\big(s_+ - 1\big)\Big[c^2 s_+\big(s_+ - 1\big) - \big(s_+\rho c + b\big)^2\Big] \tag{6}$$

As will be discussed in below, this result comes from the saddle-point-based approximation formula:

$$\sigma^2_{loc}(k,T) \approx \frac{2\frac{\partial}{\partial T}m(s,T)}{s(s-1)}\bigg|_{s=\hat{s}(k,T)} \tag{7}$$

where $\hat{s} = \hat{s}(k, T)$ is determined as the solution of the saddle-point equation:

$$\frac{\partial}{\partial s}m(s,T) = k \tag{8}$$

As such, formula (7) is clearly not restricted to the Heston model.

■ **Example: the time-dependent Black-Scholes model**. Assume

[1] *By a common abuse of notation, we write $\sigma^2_{loc}(k, T)$ instead of $\sigma^2_{loc}(S_0 \exp^k, T)$ when we wish to express the local volatility as a function of log-strike k*

risk-neutral dynamics of the form:

$$dS_t = S_t\sqrt{v(t)}dW_t$$

with $v(t)$ deterministic. We find $m(s, T) = \frac{1}{2}\, s(s-1)\int_0^T v(t)dt$, and recover $\sigma^2_{loc}(k, T) = v(T)$.

We expect our approximation formula (7) to work whenever (3) holds, assuming call prices are smooth enough to make (1) a well-defined quantity. The essence of the argument is given below. A rigorous proof in the Heston case requires some careful tail-estimates, similar to Friz *et al* (2011), and is omitted (see Friz & Gerhold, 2011). The asymptotic equivalence of (4) and (7) is shown below.

Some additional comments are in order:

- Equation (8) is solvable for large k, since (3) implies $\lim_{s\uparrow s_+}\partial/\partial s m(s, T) = \infty$.
- The solution $\hat{s}(k, T)$ to the saddle-point equation (8) can itself be used to stabilise the numerical evaluation of Dupire's formula in models with known MGF. By shifting the integration contour into the saddle point $\hat{s}(k, T) + i\mathbb{R}$, the integrands in (12) will be highly concentrated, and the performances of any numerical one-dimensional quadrature will be strongly enhanced (see figures 1 and 2, where we are using adaptive Gauss-Lobatto quadrature after shifting the integration contour).
- We have $\hat{s}(k, T) \uparrow s_+(T)$ as $k \to \infty$; hence, in models where $s_+(T) < \infty$, the denominator in (7) may be replaced by $s_+(T)(s_+(T) - 1)$. While this is correct to first order, it is often preferable to use (7) as it is, and to calculate $\hat{s}(k, T)$ by numerically solving (8). The accuracy of the resulting approximation is illustrated below for the Heston model.
- There is a version of our approximation formula (7) for small values of K, which requires that the MGF blows up at the lower critical moment $s_-(T)$. If $k < 0$ and $|k|$ is large, equation (8) has a unique solution $\hat{s}(k, T) < 0$. Then the approximation (7) holds, if $\hat{s}$ is replaced by $\hat{s}_-$.
- There are extensions of Dupire's work to jump diffusions and also pure jump models (see, for example, Bentata & Cont, 2012, and Carr *et al*, 2004). In particular, Dupire's formula becomes a partial integro-differential equation (PIDE) that features an integral term involving the second derivative of C with respect to strike, times a kernel depending on K, integrated over all strikes in $(0, \infty)$. Another difficulty in the jump setting is the potential lack of immediate smoothing. For instance, the variance gamma model satisfies the above PIDE only in the viscosity sense; in fact, call prices in the variance gamma model may not be twice differentiable in K for small times. So in a general jump setting, Dupire's formula as stated in (1), may be ill defined. And even if the call price surface is smooth enough for local volatility (1) to be well defined, the dynamics given by (2) may not be well posed, for its diffusion coefficient may be singular. Even so, it is industry standard to use Dupire's formula (1), after some smoothing of the call prices seen in the market. Since jumps cannot be ruled out from market data, this leads, unsurprisingly, to local volatility surfaces that blow up at the short end. *Ad hoc* fixes – such as freezing the volatility surface some distance away from the short end – are used in practice.

In this spirit, it is interesting to see what formula (7) gives when applied to jump models. The situation is particularly simple in exponential Lévy models, which have the property that $m(s, T)$ is linear in T and the numerator in (7) may be replaced by $2m(s, 1)$. According to the type of singularity of the MGF at the critical moment, the local volatility can display different behaviour. It is shown in Friz & Gerhold (2011) that the local variance $\sigma^2_{loc}(k, T)$ is asymptotically $c_T \times k^{1/2}$ in the double exponential Lévy model, and the constant c_T exhibits a $1/\sqrt{T}$ blow-up as $T \downarrow 0$, while it has logarithmic $\log(k/T)$ wings in the variance gamma model for large enough T. The quality of the fit obtained using (7), as well as the techniques that can be used to handle the cases of MGFs with no or slow blow-up, are also discussed in Friz & Gerhold (2011).

- The linear asymptotic behavior in (4) is likely to hold in large classes of stochastic volatility models. Relying on scaling properties and on large deviation principles, it is shown in De Marco & Friz (2012) that in the correlated Stein & Stein (1991) (or Schöbel-Zhu) model:

$$dX_t = -\frac{1}{2}\sigma_t^2 dt + \sigma_t dW_t, \quad X_0 = 0,$$
$$d\sigma_t = (a + b\sigma_t)dt + cdZ_t, \quad \sigma_0 > 0$$

the local variance is linear in the wings. To see this, set $\varepsilon^2 = 1/k$, and rescale the Stein & Stein variables as $X^\varepsilon_t = \varepsilon^2 X_t$, $\sigma^\varepsilon_t = \varepsilon\sigma_t$. Then:

$$\sigma^2_{loc}(k,T) = \mathbb{E}\left[\sigma_T^2 \,|X_T = k\right] = \varepsilon^{-2}\mathbb{E}\left[\left(\sigma_T^\varepsilon\right)^2 \middle| X_T^\varepsilon = \varepsilon^2 k\right]$$
$$= k\mathbb{E}\left[\left(\sigma_T^\varepsilon\right)^2 \middle| X_T^\varepsilon = 1\right]$$

Hence, computing $\lim_{k\to\infty}\sigma^2_{loc}(k, T)/k$ is equivalent to evaluating the asymptotics $\lim_{\varepsilon\to\infty}\sigma^2_{loc,\varepsilon}(1, T)$, where $\sigma_{loc,\varepsilon}$ is the local volatility in the rescaled problem. On the other hand, $(X^\varepsilon, \sigma^\varepsilon)$ was seen in Deuschel *et al* (2011) to satisfy a large deviation principle so that, under the above conditioning, $(X^\varepsilon, \sigma^\varepsilon)$ will centre around the least-energy path arriving at the target subspace $(1, \cdot)$ at time T, say at the point $(1, \sigma^*_T)$. Then:

$$\lim_{k\to\infty}\frac{\sigma^2_{loc}(k,T)}{k} = \left(\sigma_T^*\right)^2$$

The Pontryagin maximum principle leads to first-order optimality conditions: Hamiltonian ordinary differential equations, subject to suitable terminal and transversality conditions. Remarkably enough, these equations can be fully solved (see Deuschel *et al*, 2011), and so give σ^*_T, and hence the asymptotic slope of local variance in the Stein & Stein model explicitly in terms of the model parameters.

Saddle-point asymptotics

As is well known, we can recover the call price C and the probability density $D(\cdot, T)$ of S_T by Laplace-Fourier inversion from the MGF:

$$C(K,T) = S_0 - \frac{K}{2} + \frac{e^k}{2i\pi}\int_{-i\infty}^{i\infty} e^{-ks}\frac{M(s,T)}{s(s-1)}ds \tag{9}$$

$$D(x,T) = \frac{1}{2i\pi}\int_{-i\infty}^{i\infty} e^{-(s+1)\log x}M(s,T)ds \tag{10}$$

where the integration runs over the imaginary axis $i\mathbb{R}$. Now differentiate the call price with respect to maturity under the integral sign:

$$\partial_T C(K,T) = \frac{e^k}{2i\pi}\int_{-i\infty}^{i\infty}\frac{\partial_T m(s,T)}{s(s-1)}e^{-ks}M(s,T)ds \tag{11}$$

By Dupire's formula, we have:

$$\sigma^2_{loc}(k,T) = \frac{2\partial_T C(K)}{K^2 D(K,T)} = \frac{2\int_{-i\infty}^{i\infty}\frac{\partial_T m(s,T)}{s(s-1)}e^{-ks}M(s,T)ds}{\int_{-i\infty}^{i\infty}e^{-ks}M(s,T)ds} \tag{12}$$

Both integrands in (12) have a singularity at $s = s_+$, since $M(s, T)$ blows up there. The singular behaviour of $M(s, T)$ dominates the asymptotics of both integrals. The resulting asymptotic factor cancels, and only the contribution of $2(\partial_T m(s, T))/(s(s-1))$ remains. This is the idea behind (7).

To implement it, we analyse both integrals in (12) by a saddle-point approximation. If M features an exponential blow-up at the critical moment s_+, its validity can be justified rather universally. Examples include the Heston model, double exponential Lévy and Black-Scholes. If the saddle-point method is not applicable, different arguments are required (see section 3 of Friz & Gerhold, 2011).

So let us proceed with the saddle-point analysis of (12). For both integrals, we only use the factor $e^{-ks}M(s)$ to find the location of the (approximate) saddle point $\hat{s} = \hat{s}(k, T)$. The saddle-point equation is (8), obtained by equating the derivative of $e^{-ks}M(s)$ to zero. We move the integration contour through the saddle point. Then, for large k, only a small part of the contour, around the saddle point, with $|\Im(s)| \le h(k)$ for some function $h(k)$ dependent on the expansion – for example $h(k) = k^{-5/7}$ in the Heston case – matters asymptotically. The integral can be approximated via a local expansion of the integrand. Let us carry this out for the denominator of (12), writing a prime for differentiation with respect to s. We have:

$$\begin{aligned}
&\int_{\hat{s}-i\infty}^{\hat{s}+i\infty} e^{-ks}M(s,T)\,ds \sim \int_{\hat{s}-ih(k)}^{\hat{s}+ih(k)} e^{-ks}M(s,T)\,ds \\
&\sim \int_{\hat{s}-ih(k)}^{\hat{s}+ih(k)} \exp\Big(-ks + m(\hat{s},T) + k(s-\hat{s}) + \tfrac{1}{2}m''(\hat{s},T)(s-\hat{s})^2\Big)\,ds \qquad (13)\\
&= e^{m(\hat{s},T)-k\hat{s}} \int_{\hat{s}-ih(k)}^{\hat{s}+ih(k)} \exp\Big(\tfrac{1}{2}m''(\hat{s},T)(s-\hat{s})^2\Big)\,ds
\end{aligned}$$

using $m'(\hat{s}, T) = k$ in the Taylor expansion of the exponent. Now the crucial observation is that the numerator of (12) admits a similar approximation, where the only new ingredient is the factor $2(\partial_T m(s, T))/(s(s-1))$:

$$\begin{aligned}
&2\int_{-i\infty}^{i\infty} \frac{\partial_T m(s,T)}{s(s-1)} e^{-ks}M(s,T)\,ds \\
&\sim 2\int_{\hat{s}-ih(k)}^{\hat{s}+ih(k)} \frac{\partial_T m(s,T)}{s(s-1)} e^{-ks}M(s,T) \\
&\sim 2e^{m(\hat{s},T)-k\hat{s}} \int_{\hat{s}-ih(k)}^{\hat{s}+ih(k)} \frac{\partial_T m(\hat{s},T)}{\hat{s}(\hat{s}-1)}\big(1+o(1)\big)\exp\Big(\tfrac{1}{2}m''(\hat{s},T)(s-\hat{s})^2\Big)\,ds \qquad (14)\\
&\sim 2\frac{\partial_T m(\hat{s},T)}{\hat{s}(\hat{s}-1)} e^{m(\hat{s},T)-k\hat{s}} \int_{\hat{s}-ih(k)}^{\hat{s}+ih(k)} \exp\Big(\tfrac{1}{2}m''(\hat{s},T)(s-\hat{s})^2\Big)\,ds
\end{aligned}$$

Dividing (14) by (13) concludes the derivation. Summarising, we note that the asymptotics of $\sigma^2_{loc}(k)$ are governed by the local expansions at $s = \hat{s}$ of the integrands in (12). The respective first terms of both expansions agree, and thus cancel, except for the factor (7).

Local volatility at extreme strikes in the Heston model

Here, we focus on the Heston model, testing our approximation formula and asymptotic result, and explaining how (4) is obtained by specialising (7).

Note that the saddle-point based approximation (7) provides an almost explicit formula for the local volatility in the Heston model. The right-hand side of (7) can be easily evaluated using the explicit expression of the Heston MGF. The evaluation of the saddle point $\hat{s}(k, T)$ requires the inversion of the derivative $\partial_s m(s, T)$ (again explicit) in (8). This root-finding can be performed by simple bisection or by Newton-Raphson, the latter method allowing explicit approximate expression of the saddle point (20). Table B shows that the number of iterations involved in this root-finding procedure stays bounded – and small – across maturities and log-moneyness.

B. Saddle-point approximation

Maturity	Number of function evaluations	
	Minimum	Maximum
0.25	7	8
1	7	9
10	11	12

Note: number of evaluations of $\partial_s m(s, T)$ required to find the saddle point $\hat{s}(k, T)$ with a relative precision of 10^{-8}, using Newton-Raphson and starting from the explicit approximate saddle point $\hat{s}$ in (20). The number of function evaluations sampled over k range from 0.1 to 3

3 Boundaries of the region R_e in (15)

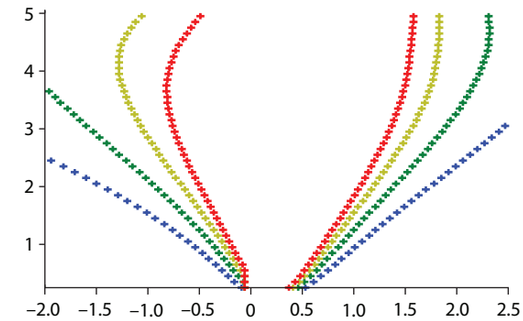

Note: boundaries of the region R_e in (15) for e = 2% (blue), 3% (green), 4% (yellow), 5% (red). Heston parameters are as in figure 4; maturities range down to $T = 0.25$

We use the approximation formula (7) as follows: one starts by identifying a region $\hat{R}$ in the (k, T) plane where a reliable numerical implementation $\hat{\sigma}^2_{loc}(k, T)$ of the local variance is available. Typically, the software system of an option trading desk will allow one to do so, when fed with Heston call prices (in trusted regimes). We may assume that the numerical evaluation of $\hat{\sigma}^2_{loc}(k, T)$ comes with a relative error bound E_1. On the boundary of $\hat{R}$, one compares the value of $\hat{\sigma}_{loc}$ with the output of formula (7), computing the relative accuracy:

$$E_2 = \left|\hat{\sigma}^2_{loc}(k,T) - \frac{\partial_T m(s,T)}{s(s-1)}\bigg|_{s=\hat{s}(k,T)}\right| \Big/ \hat{\sigma}^2_{loc}(k,T)$$

If the approximation formula (7) is used to replace the numerical evaluation of $\hat{\sigma}_{loc}$ on the outer region, the complement of $\hat{R}$, the resulting globally defined local variance surface will have a relative accuracy of approximately $E_1 + E_2$. When the relative precision E_2 observed on the boundary is too large to be considered acceptable, the region $\hat{R}$ needs to be extended. This amounts to improving on the existing software, so one cannot be more specific. The trade-off between numerical and approximation accuracies E_1 and E_2 is set according to user preferences – in order to illustrate here the accuracy of the saddle-point formula (7) in the (k, T) plane, in figure 3 we plot the boundaries of the regions:

$$R_e = \left\{(k,T): \frac{\left|\hat{\sigma}^2_{loc}(k,T) - \frac{\partial_T m(s,T)}{s(s-1)}\Big|_{s=\hat{s}(k,T)}\right|}{\hat{\sigma}^2_{loc}(k,T)} < e\right\} \qquad (15)$$

4 Local variance $\sigma^2_{loc}(k, T)$ (left and right wing) in the Heston model

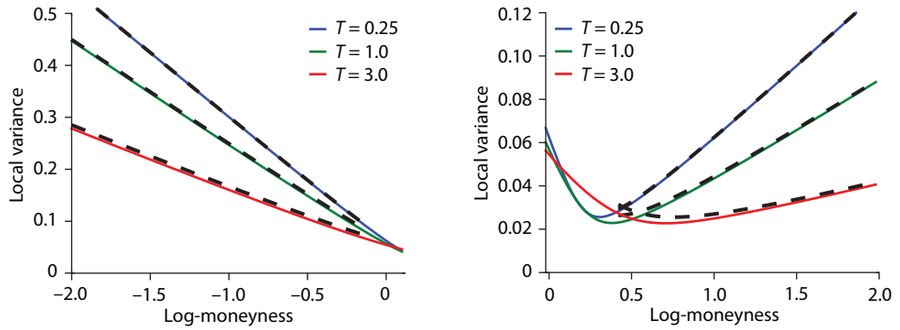

Note: parameters are $a = 0.0428937$, $b = -0.6067$, $c = 0.2928$, $s_0 = 1$, $v_0 = 0.0654$, $\rho = -0.7571$. The solid lines show the local variance calculated with Dupire's formula and adaptive integration contour as in figures 1 and 2. The approximation (7) is dashed

5 Implied volatilities generated by the Heston local volatility

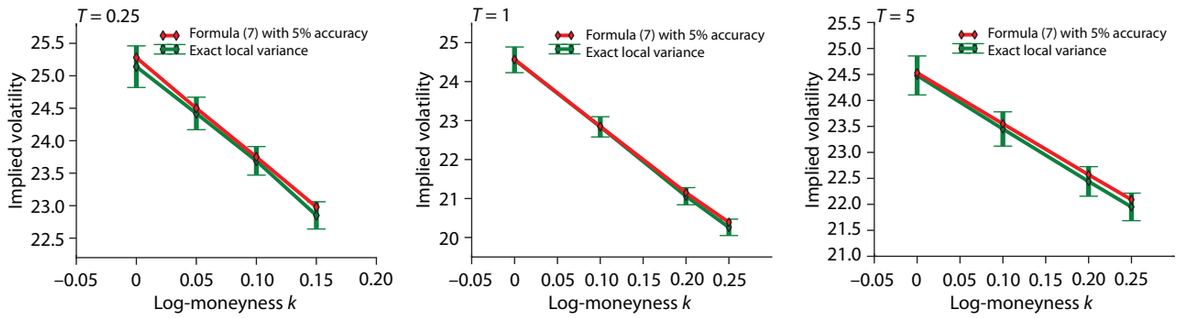

Note: implied volatilities generated by the Heston local volatility calculated via Dupire's formula and adaptive integration contour in (12) (green curve), and when this numerical evaluation is replaced with the approximation formula (7) on the region R_e, $e = 5\%$ (figure 3 outside the red boundaries) (red curve). The error bars show the 95% confidence interval for the simulation under exact local variance. Monte Carlo parameters: 12 time steps a year (16 for shortest maturity), 5×10^4 trajectories

for values of e ranging from 2% (blue boundary) to $e = 5\%$ (red boundary). In each case, R_e is the outer region in the figure. Here $\hat{\sigma}^2_{loc}(k, T)$ is evaluated using Dupire's formula (12) after shifting the integration contour into the saddle point $\hat{s}(k, T) + i\mathbb{R}$, then using a one-dimensional adaptive Gauss-Lobatto quadrature with an high precision (as described above), so that the relative error in the evaluation of $\hat{\sigma}^2_{loc}(k, T)$ is negligible with respect to e. In its turn, figure 4 compares the value of $\hat{\sigma}^2_{loc}$ calculated according to this procedure and:

$$\left.\frac{\partial_T m(s,T)}{s(s-1)}\right|_{s=\hat{s}(k,T)}$$

The convergence of the approximation in the outer region, together with the good fit in a wide range of strikes, is clearly seen, in particular for short maturities.

We now investigate the impact of our local volatility approximation on option prices, given in terms of implied volatility. Clearly, when the local volatility is replaced with the saddle-point-based approximation (7) in the wings, we are expecting a good fit of the implied volatility output. Figure 5 compares the implied volatilities obtained by Monte Carlo under Heston local volatility calculated via Dupire's formula and adaptive integration contour in (12), as in the right panel of figures 1 and 2, with local volatility replaced by formula (7) on the region R_e, $e = 5\%$. The smile obtained when formula (7) is taken into account (red curve) is indeed very accurate, as it lies within the 95% confidence interval of the simulation done under the exact local variance (green curve).

We will now show that the right-hand side of (7) is indeed asymptotically equivalent to the right-hand side of (4). This requires us to show that:

$$2\frac{\partial}{\partial T}m(s,T)\Big|_{s=\hat{s}(k,T)} \sim 2k/\sigma \tag{16}$$

where $\sigma = \sigma(T)$ is the so-called critical slope, defined as:

$$\sigma(T) = -\frac{\partial T^*}{\partial s}\left(s_+(T)\right), \qquad T^*(s) = \sup\left\{t \geq 0 : \mathbb{E}\left[e^{sX_t}\right] < \infty\right\} \tag{17}$$

In fact, while the calculation of the critical exponent s_+ in the Heston model requires simple numerics, the critical slope can be calculated in closed form (Friz *et al*, 2011). We have $\sigma(T) = R_1/R_2$, where $R_i = R_i(b, c, \rho, s_+(T))$, $i = 1, 2$, are defined in (5) and (6).

Since $\hat{s}(k, T) \to s_+(T)$ as $k \to \infty$, if (16) is verified, the right-hand side of (7) then satisfies:

$$\left.\frac{2\frac{\partial}{\partial T}m(s,T)}{s(s-1)}\right|_{s=\hat{s}(k,T)} \sim \frac{2}{\sigma(T)s_+(T)\left(s_+(T)-1\right)}\times k, \quad k\to\infty$$

which is the formula from our theorem. Let us now discuss the validity of (16). The argument that follows nicely illustrates how formula (7) can be used in stochastic volatility models of affine type. From an asymptotic analysis of the Riccati equations (Friz *et al*, 2011), writing $s_+ = s_+(T)$ when T is fixed, $m(s,t)$ is known to satisfy:

$$m(s,t) \sim \frac{v_0}{\frac{c^2}{2}\sigma\left(s_+ - s\right)}, \quad s \uparrow s_+$$

$$\frac{\partial}{\partial s}m(s,t) \sim \frac{v_0}{\frac{c^2}{2}\sigma\left(s_+ - s\right)^2}, \quad s \uparrow s_+ \tag{18}$$

$$\frac{\partial}{\partial T}m(s,T) \sim \frac{v_0}{\frac{c^2}{2}\left(\sigma\left(s_+ - s\right)\right)^2}, \quad s \uparrow s_+ \tag{19}$$

Equation (8) leads to:

$$\hat{s} = s_+ = \beta k^{-1/2} + o\left(k^{-1/2}\right) \tag{20}$$

since:

$$\frac{\partial}{\partial s}m(s,t) \sim \frac{v_0}{\frac{c^2}{2}\sigma\left(s_+ - \hat{s}\right)^2} = k \Rightarrow s_+ - \hat{s} \sim \beta k^{-1/2}$$

with:

$$\beta = \frac{\sqrt{2v_0}}{c\sqrt{\sigma}}$$

Substitution then yields:

$$\left.\frac{\partial}{\partial T}m(s,T)\right|_{s=\hat{s}} \sim \frac{v_0}{\frac{c^2}{2}\sigma^2\beta^2/k} = k/\sigma$$

which concludes our derivation of (16).

A numerical example of the convergence of the slope of the left-wing local variance $\sigma^2_{loc}(k,T)/k$ to its asymptotic value is shown in figure 6.

6 Convergence of the slope of local variance to its asymptotic value ($k < 0$)

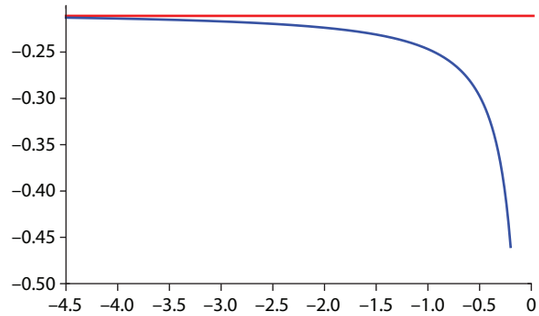

Note: blue line: $k \mapsto (\sigma^2_{loc}(k,T))/k$, $T = 1$. Red line: asymptotic value from (4). Heston parameters as in figure 4. This gives numerical confirmation of the analytic result (9). For actual numerics, the approximation formula (7) is preferred

Conclusion

We have proposed a new formula that expresses local volatility for extreme strikes as a calculable function of commonly available model information. In the Heston model, this leads to a proof that local variance behaves asymptotically linearly in log-strike, qualitatively similar to Lee's result (2004) for implied volatility. This suggests concrete parameterisations of the local volatility surface. In contrast to *ad hoc* specifications of the implied volatility surface, there is no danger of introducing arbitrage. We also investigated the form of local volatility defined via Dupire's formula when the underlying exhibits jumps; qualitatively different behaviour (compared with diffusion models such as Heston) is seen.

Our results also help the process of quantifying model risk for path-dependent options. Indeed, as we explained in the introduction, using our formula local volatility surfaces can be constructed in a globally robust fashion. Prices of exotic options under local volatility can then be compared with the prices obtained in the matching stochastic volatility model.

All asymptotics results are supported by numerical examples based on our novel and generic approximation formula (7). ■

Stefano de Marco is assistant professor in applied mathematics at the Ecole Polytechnique in Paris. Peter Friz is professor in mathematics at TU and WIAS in Berlin. Stefan Gerhold is assistant professor in mathematics at TU in Vienna.
Friz would like to thank Rama Cont, Bruno Dupire and Jim Gatheral for related discussions. Participants of Global Derivatives 2012 (Barcelona), where this work was first presented, are also thanked for their interest. The numerical tests have been built on top of the Zeliade Systems analytic framework ZQF.
Email: stefano.de.marco@cmap.polytechnique.fr, friz@math.tu-berlin.de, friz@wias-berlin.de, sgerhold@fam.tuwien.ac.at

References

Bentata A and R Cont, 2012
Forward equations for option prices in semimartingale models
Forthcoming in Finance and Stochastics

Carr P, H Geman, D Madan and M Yor, 2004
From local volatility to local Lévy models
Quantitative Finance 4, pages 581–588

De Marco S and P Friz, 2012
Varadhan's formula for projected diffusions and local volatility
Working paper

Deuschel J-D, P Friz, A Jacquier and S Violante, 2011
Marginal density expansion for diffusions and stochastic volatility, part I and II
Forthcoming in Communications on Pure and Applied Mathematics

Dupire B, 1994
Pricing with a smile
Risk July, pages 18–20, available at *www.risk.net/1530409*

Friz P and S Gerhold, 2011
Don't stay local – extrapolation analytics for Dupire's local volatility
Preprint, available at *http://arxiv.org/abs/1105.1267*

Friz P, S Gerhold, A Gulisashvili and S Sturm, 2011
On refined volatility smile expansion in the Heston model
Quantitative Finance 11, pages 1,151–1,164

Gatheral J, 2006
The volatility surface, a practitioner's guide
Wiley

Gatheral J and A Jacquier, 2012
Arbitrage-free SVI volatility surfaces
SSRN working paper, available at *http://ssrn.com/abstract=2033323*

Lee R, 2004
The moment formula for implied volatility at extreme strikes
Mathematical Finance 14, pages 469–480

Reghai A, 2011
Model evolution
Presentation at the Parisian Model Validation seminar, available at *https://sites.google.com/site/projeteuclide/les-seminaires-vmf/archives-vmf*

Stein E and J Stein, 1991
Stock price distribution with stochastic volatility: an analytic approach
Review of Financial Studies 4, pages 727–752